Ingeniería y Competitividad
Vol 27 (3) 2025 doi: 10.25100/iyc.v27i3.14972

Vol 27 (3)

ISSN
0123-3033
e- 2027-8284

Original Article

Characterization of white and brown etching layers promoted by a small-scale grinding process in laboratory

Caracterización de capa blanca y marrón promovidas por un proceso de esmerilado a baja escala en laboratorio

J.C. Sánchez[1] J.A. Jaramillo[1] H. Estupiñán[1] G. Hernández[1]
A. Toro[1] V. Wilches[1]

[1]Energy Research and Innovation Group – GIIEN, Institución Universitaria Pascual Bravo, Medellín Colombia
[2] Tribology and Surfaces Group, Universidad Nacional de Colombia, Medellín, Colombia
[3] Materiales y Procesos Altenativos MAPA, Universidad EIA, Envigado, Colombia

Abstract

Objectives: The main objective of this study was to promote the formation of White and Brown Etching Layers (WEL and BEL) on R260 pearlitic steel by means of a controlled laboratory grinding process, in order to analyze the microstructural and mechanical changes from the surface to the base material.
Materials and methods: R260 pearlitic steel used for railway rail manufacturing was investigated. The transformed surface layers were generated through a controlled grinding process. Microstructural characterization was performed using light optical microscopy (LOM) and scanning electron microscopy (SEM). Mechanical characterization was carried out by micro-hardness testing and nanoindentation from the ground surface toward the bulk material. Subsequently, the WEL region was analyzed by transmission electron microscopy (TEM) to identify microstructural changes in the different zones affected by the grinding process.
Results: The results showed that WEL and BEL can be distinguished not only by their morphological features observed by LOM and SEM, but also by their mechanical properties. Both layers exhibited significantly higher hardness and Young's modulus values than the pearlitic base material.
Conclusions: The microstructural transformations induced by the grinding process were visually identified as WEL and BEL through contrast and texture variations observed by LOM and SEM. These layers extended from the ground surface to depths of approximately 30 µm and exhibited distinct mechanical responses associated with intrinsic microstructural changes generated by the grinding process.

Keywords: WEL, BEL, Grinding, Pearlite, Mechanical properties.

Resumen

Objetivos: El objetivo principal de este estudio fue promover la formación de capas de ataque blanco y marrón (White Etching Layer, WEL, y Brown Etching Layer, BEL) en acero perlítico R260 mediante un proceso de rectificado controlado en laboratorio, con el fin de analizar los cambios microestructurales y mecánicos desde la superficie hasta el material base.
Materiales y métodos: Se utilizó acero perlítico R260 empleado en la fabricación de rieles ferroviarios. Las capas transformadas se generaron mediante un proceso de rectificado controlado. La caracterización microestructural se realizó mediante microscopía óptica (LOM) y microscopía electrónica de barrido (SEM). La caracterización mecánica se llevó a cabo mediante ensayos de microdureza y nanoindentación desde la superficie rectificada hacia el volumen del material. Posteriormente, la zona WEL fue analizada mediante microscopía electrónica de transmisión (TEM) para identificar los cambios microestructurales en las diferentes zonas afectadas por el rectificado.
Resultados: Los resultados mostraron que es posible distinguir la WEL de la BEL no solo por sus características morfológicas observadas mediante LOM y SEM, sino también por sus propiedades mecánicas. Ambas capas presentaron valores de dureza y módulo de Young significativamente superiores a los del material base perlítico.
Conclusiones: Las transformaciones microestructurales inducidas por el rectificado se identificaron visualmente como WEL y BEL a través de variaciones en el contraste y la textura observadas mediante LOM y SEM. Estas capas se extendieron desde la superficie rectificada hasta profundidades cercanas a 30 µm y presentaron respuestas mecánicas diferenciadas, asociadas a cambios microestructurales intrínsecos generados por el proceso de rectificado.

Palabras clave: WEL, BEL, Molienda, Perlita, Propiedades mecánicas.

How to cite?

Sánchez JC, Jaramillo JA, Estupiñán H, Hernández G. Characterization of white and brown etching layers promoted by a small-scale grinding process in laboratory. Ingeniería y Competitividad, 2025, 27(3)e-21014972

https://doi.org/10.25100/iyc.v27i3.14792

Received: 07/07/25
Reviewed: 06/10/25
Accepted: 1/12/25
Online: 19/01/26

Correspondence

juan.sanchezg@pascualbravo.edu.co

Spanish version

Why was this study conducted?
This topic is currently of critical relevance to the railway sector, as it represents a primary damage mechanism on rail heads that leads to significantly shortened maintenance intervals. Furthermore, elucidating the properties and potential formation mechanisms can facilitate adjustments in operating conditions to prevent the premature formation of this layer, thereby aiding in the development of effective mitigation strategies

What were the most relevant findings?
The study achieved the distinct formation of a microstructure under controlled laboratory conditions, which presents a marked visual contrast against the base material. The resulting phase exhibited mechanical and elastic property values up to a fourfold increase compared to the initial microstructure. Additionally, a transition zone was evidenced between the bulk material and the contact surface where the WEL developed, displaying intermediate mechanical and elastic properties relative to the other two microstructures.

What do these findings contribute?
This work provides a reproducible method to promote White Etching Layer (WEL) formation on rail heads under controlled laboratory conditions. This serves as a foundational step for predicting or validating the formation mechanisms of this microstructure in railway systems under operating conditions

Graphical Abstract

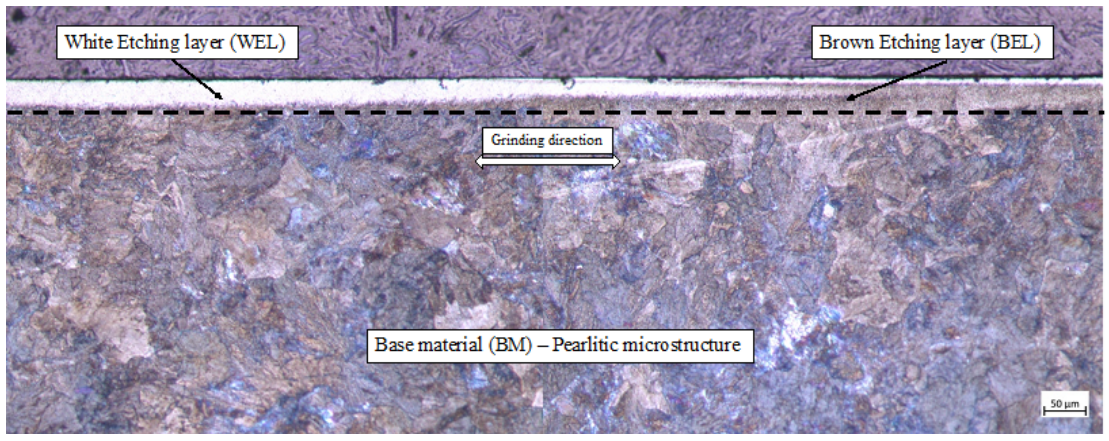

doi: 10.25100/iyc.v27i3.14972

Introduction

The high and repetitive external loading conditions registered in wheel / rail pairs of railway systems, generate accumulative surface alterations in the contact areas and nearby regions. The continue contact with the wheel promotes several phenomena that in some cases do not contribute with a good performance of the rail under commercial operation conditions. Some of them problems have been shown in research before as squats (1–3), studs (4,5) , cracks by RCF (6–8) , corrugation (9–11) or WEL (12–14) the which are associated to many aspects and variables such as load (15) , creepage (16–18), chemical composition and microstructure (19,20) etc., by promoting in some cases catastrophic damages on the railway. One of these problems associate to the contact that has been focus of several researches in the last years is the WEL, both its performance and its formation mechanisms (21–23). Several researches have been carried out in relation to this topic not only for railway systems but other components and fields also like rolling bearings (24,25) , machining process (26,27) etc. However, in railway systems, the formation of this layer is related to other rail's damages as squats or RCF mechanism (28,29) by promoting microcracking inside the rail (30–33) that could cause a complete fracture of the component and high maintenance costs (5,34,35). The phases present in this zone have different hypotheses about the microstructure: martensite (36) , Fe-C nanocrystals (37), deformed pearlite, martensite nanocrystals, austenite and cementite (38). The formation of the WEL has been evidenced in commercial activities, rail-wheel contact, and grinding activities of maintenances and according to this, two hypotheses about the formation of the WEL have been proposed by several researchers: (1) the first one has been related with the microstructural changes associated with the high temperatures reaches in the contact between rail-wheel and rail-grinding stone (36,39,40) and (2) the second one has been associated with the high plastic deformation the which is promoted by the high tangential forces on the contact area (37,41–43). According to the first hypothesis, the temperatures reached in the process exceed the autenization temperature and the rapid cooling promotes the martensitic transformation that is corroborated with hardness measurements made on the layer and in some cases is confirmed by retained austenite zones found that support this assumption. With relation of the second hypothesis, the phenomenon is associated with the dissolution of the pearlitic microstructure. Inside of the pearlitic grains, the cementite is dissolved by the high stresses and dislocations movements and the carbon atoms enriched the carbon amounts of the ferrite by increasing its mechanical properties. This could be supported by TEM's images the which show diffraction patterns of nano-grains (22,44). Confirming this hypothesis allows to create strategies not only for improving the tribological behavior by reducing the tangential force but also to reduce the temperature in the interface.

In additions, it has been shown that between the WEL and pearlite substrate it is possible find a new microstructure with intermediate mechanical properties can be formed the which is identified by its brown color when is etched by Nital 3% and observed by light optical microscopy (45) and from this, the layer is called BEL (Brown Etching Layer). Its formation is related by two explanations: (1) the first is associated with a microstructure transition in the process of the WEL formation and because of this its mechanical properties are between the WEL and the pearlite, (2) the other one is explained as a tempered martensite after WEL formation caused by the thermal cycles on the contact interface.

doi: 10.25100/iyc.v27i3.14972

In this work is evaluated the possibility of promoting the WEL formation in laboratory on a commercial rail section by grinding process on a small scale for measuring optical microstructure changes and its mechanical properties in comparison with the base material of the component that is a pearlitic microstructure. Samples on the grinding surface were extracted for the optical inspection by LOM and SEM and for mechanical characterization microhardness and nanoindentation were made. The values obtained were correlated with the microstructures observed and are associated with the hypothesis proposed in the literature.

Furthermore, this study validates the formation of a White Etching Layer (WEL) on rail running surfaces under grinding conditions. This finding is a crucial step toward implementing advanced techniques to characterize changes in the rail head, specifically the altered microstructure and material properties resulting from wheel-rail contact. Therefore, the ability to induce WEL formation in the laboratory will be highly beneficial as a preliminary step for the development and calibration of Non-Destructive Testing (NDT) methods to support new maintenance strategies in this field as identification stage of damages promote by microstructural changes on the contact surface

Materials and methods

Material

The material used was a pearlitic steel for manufacturing rails with the designation R260. The chemical composition is shown in Table 1 and the microstructure is shown in Fig. 1.

Table 1. Chemical composition (wt.%) of the rail material used for the tests.

Element	C	Si	Mn	S	P	Ni	Cr	Mo	Al	Cu	Pb	Sn	Ti	V	Sb	Ca
wt.%	0.736	0.27	1.056	0.023	0.032	0.021	0.026	0.006	0	0.002	0	0	0.016	0.003	0	0

Figure 1. Microstructure of the rail material R260. SEM. (2000x). Pearlitic steel.

doi: 10.25100/iyc.v27i3.14972

The microstructure shown in Figure above shows a micrograph completely pearlitic according to the chemical composition shown in Table 1 which classifies the material as eutectoid steel.

WEL formation process

The formation of a white etching layer on the surface of the rail material was promoted by a grinding process. An industrial machine was adapted to simulate small scale conditions of a grinding process in a commercial railway. Fig. 2 shows the arrangement used for testing.

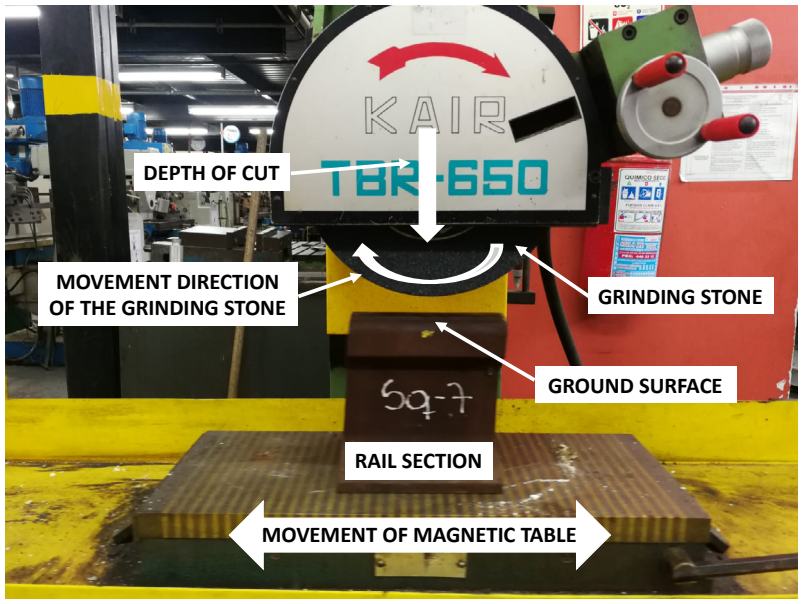

Figure 2. Machine used for promoting the WEL formation on the rail material surface

The conditions of the process considered were as follows: velocity of grinding stone of 2120 rpm, 30 µm of cutting depth , 1 m/s of linear velocity of the magnetic table and just one pass of the stone on the rail head. The load value was set in static conditions by placing a load cell under the sample. The variation of the load as a function of the cutting depth was determined experimentally as shown in Fig. 3, where it can be seen that for a depth of cut of 30 µm the static load is around 160 gf.

doi: 10.25100/iyc.v27i3.14972

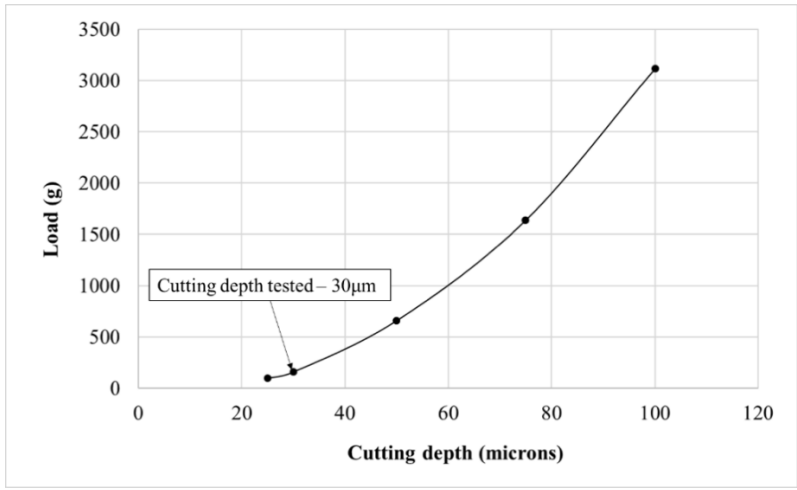

Figure 3. Experimental estimation of the maximum load as a function of the cutting depth

Optical characterization

The analysis of the WEL was made by using a ZEISS Axioscope 5 LOM and a ZEISS EVO 10 SEM with a voltage of 20kV and a work distance less 9mm.. Longitudinal (L) sections were extracted from the rail head as shown in Fig. 4. Also, a characterization by TEM was made to confirm the microstructure generated on the contact surface by the grinding process. For TEM analysis, thin foils were prepared through focused ion beam (FIB) in Brazilian Center for Research in Energy and Materials (CNPEM). The specimens were examined using a JEOL JEM-2100F multipurpose analytical electron microscope equipped with a field emission gun (FEG) operating at 200 kV. Analyses of several specimens were performed using electron diffraction patterns obtained through selected area electron diffraction (SAED) mode at various locations within the inspection area, utilizing the same camera length. The metallographic preparation of the samples was carried out following the ASTM E3 procedure and etching was carried out with Nital 3%.

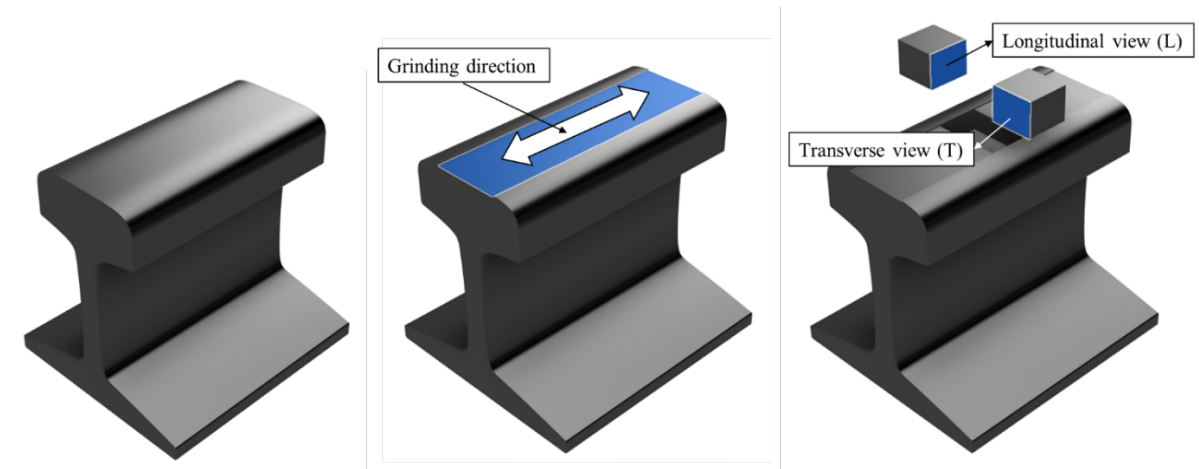

Figure 4. Extraction zone of the samples analyzed.

doi: 10.25100/iyc.v27i3.14972

Mechanical characterization

Microhardness tests in SHIMANU HMV-G31 and nano indentation tests in Ibis Authority- Fischer Cripps Laboratories were carried out to study the variation of mechanical properties with respect to the distance to the surface.

Results and discussion

Optical microstructural analysis

Fig. 5 shows the microstructure obtained after the grinding process. A white etching layer (WEL) formed at the surface due to the contact with the grinding stone and a brown etching layer (BEL), which has been reported by other authors (37,46–49) can also be observed. Although the thicknesses of the WEL and BEL vary over the contact surface, it seems that the overall thickness of the material affected by the thermomechanical process remains stable (see the dotted line in the figure).

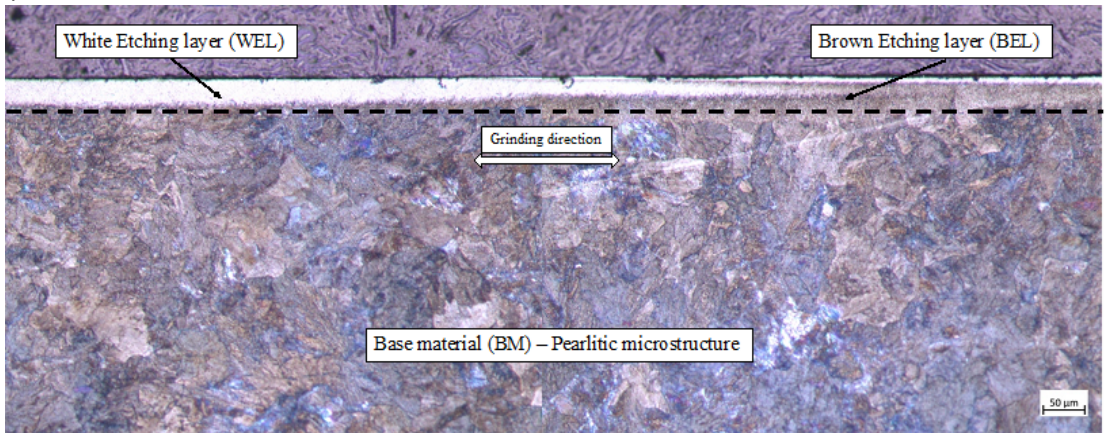

Figure 5. Cross-sectional view of the microstructure after grinding process. Longitudinal view

Fig. 6 shows in more detail the microstructure of a ground sample examined by SEM. While the WEL is homogeneous and shows little electronic contrast, the BEL has the aspect of being composed of fractured pearlitic lamellae, which is consistent with the high tangential forces on the interface between rail and grinding stone (41,48,50,51). The zone analyzed was taken near to the contact zone to ensure the identification of microstructural changes.

doi: 10.25100/iyc.v27i3.14972

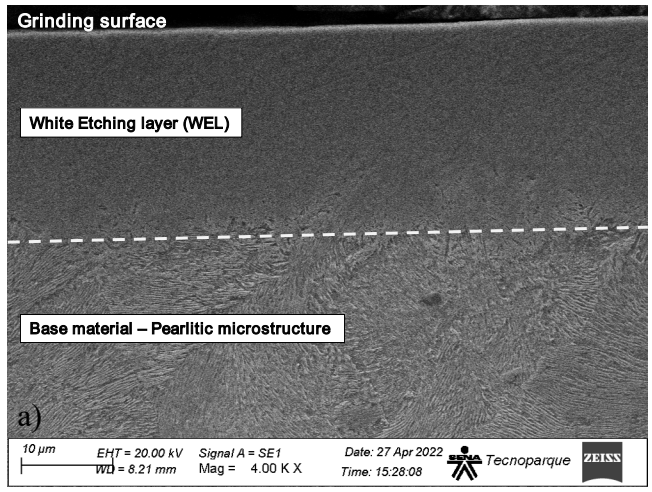

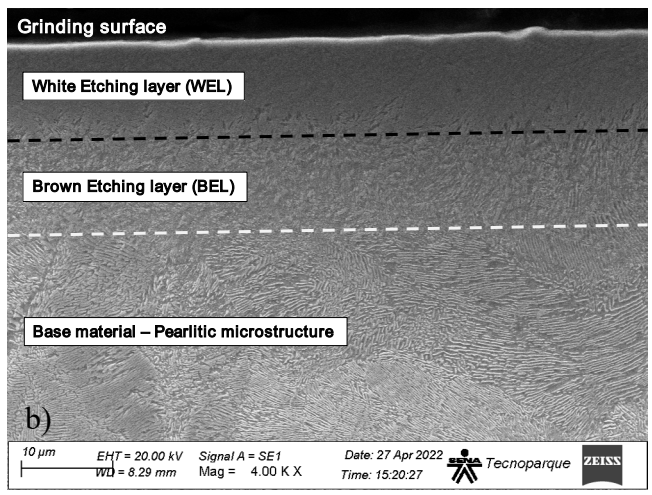

Figure 6. Microstructural variation from the ground surface to the substrate (4000x**).** Longitudinal view

From Fig. 6a) and 6b) it can be corroborated that the microstructure in the subsurface has a variation concerning the depth as it was shown above. In addition, like it said before, it can be identified a variation of the two first zones concerning to the transformed layer (WEL and BEL). From this, in Fig. 6a) an imaginary line was established to separate these zones with respect to the pearlitic base material for identifying the thermal and plastic affected zone by the grinding process. In both images, Fig. 6a) and 6b), the white dotted line, which separates the transformed microstructure, is positioned at the same depth of around 30 microns and it does not change in both cases, however, the black dotted line, that separates the WEL and BEL (Fig. 6b), shows a variation of the WEL amount transformed as it was identified in Fig. 5, by suggesting possible hypothesis of a limit quantity of the transformed material for specific test conditions of grinding process.

Microhardness and nano-indentation

Fig. 7 shows the results of microhardness measurements as a function of the distance from the contact surface.

doi: 10.25100/iyc.v27i3.14972

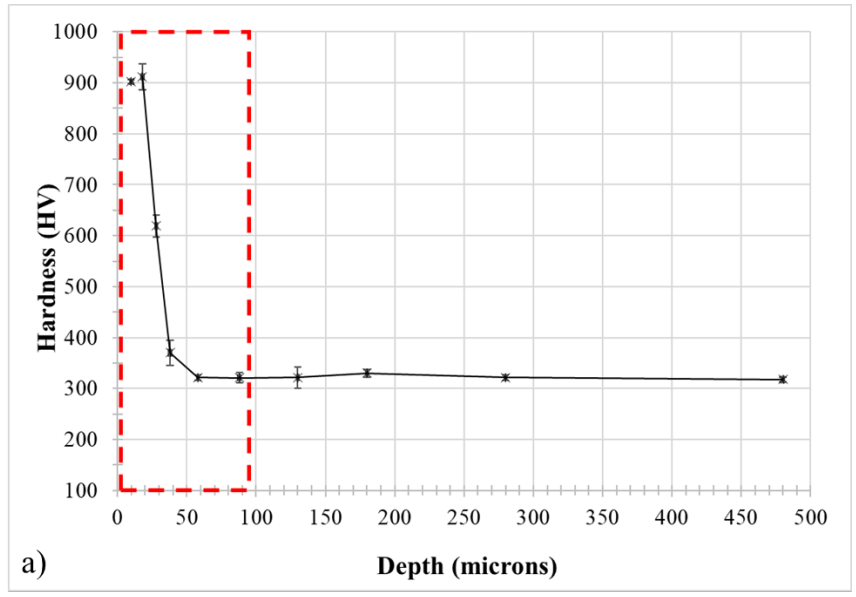

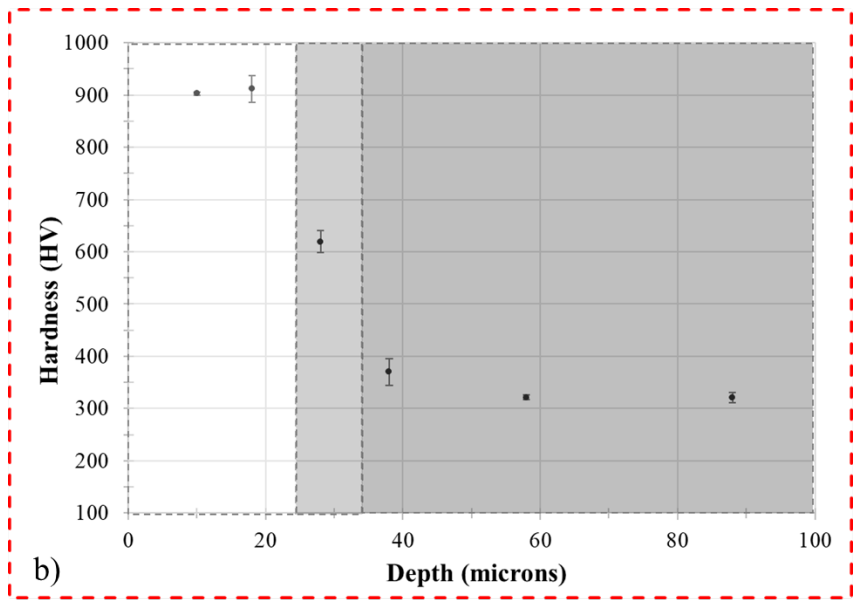

Figure 7. Microhardness results of a cross section after grinding process. a) Microhardness profile in function of distance to the surface, b) Detail of the first 100 microns from the surface.

The results obtained show a marked increase of the hardness near to the contact surface in comparison with the values shown in the pearlitic microstructure by decreasing when the depth rises from the ground surface. Fig. 7b) allows identifying the three zones (WEL, BEL and base material) according to their microhardness values, i.e. 910HV for WEL, 640HV for BEL and 310HV for pearlite. These values are in agreement with data reported by other authors for similar structures (25,38,42,43,52).

Fig. 8 shows the values of hardness (H) and Young's modulus (E) for each zone measured by nanoindentation tests. As expected, both H and E decrease with the distance to the surface with respect to the microstructural variation. The data for the three zones are similar to the results

doi: 10.25100/iyc.v27i3.14972

reported by other authors (43,50,53) who reported values around to 11 - 13 GPa for WEL, 5 - 6.5 GPa for BEL and 3.5-4.5 GPa for the pearlitic structure (base material).

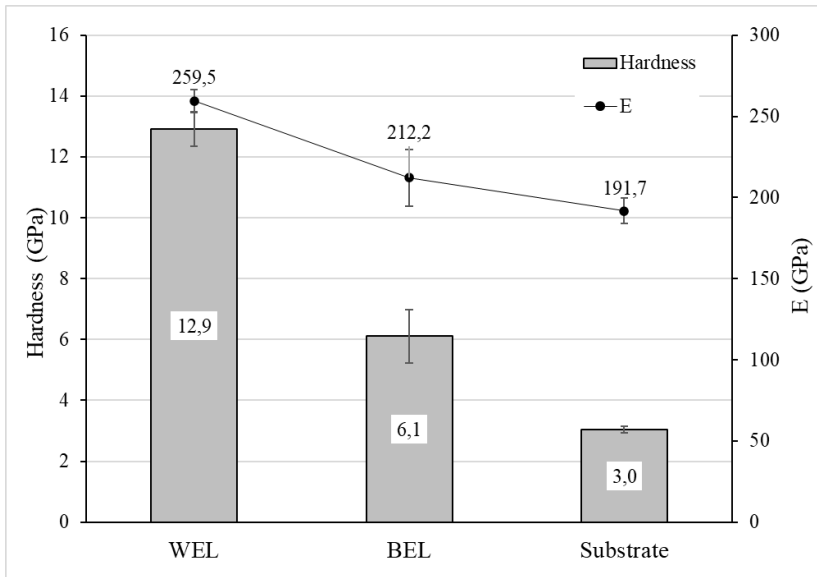

Figure 8. Hardness and Young's modulus for WEL, BEL and base material. Nanoindentation measurements.

Fig. 9 presents a visual description of the variation of microhardness measured parallel to the contact surface along the white and brown etching layers. The indentations were made in a part of the section shown in Fig. 5 where the variation between WEL and BEL can be identified visually.

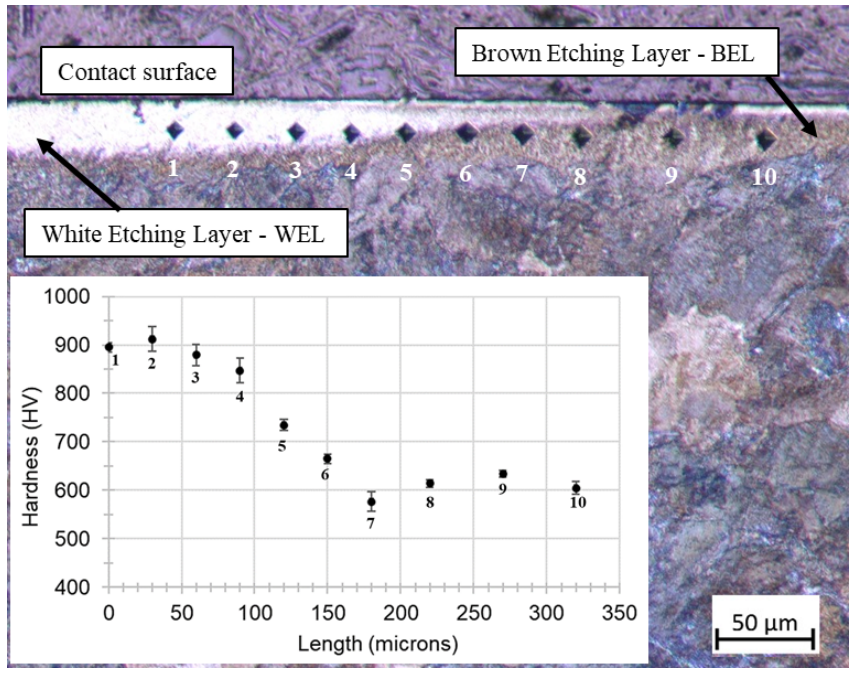

Figure 9. Microhardness profile in the affected zone by the grinding process. Longitudinal view

doi: 10.25100/iyc.v27i3.14972

The results confirmed that both, WEL and BEL, have different mechanical properties associated with values reported before and is possible that the WEL transformed reaches a maximum layer thickness associated with the grinding conditions been the BEL a previous microstructure to its transformation(54–56).

Also, a microstructural analysis was performed using TEM to identify the microstructure of the WEL and to corroborate the preliminary hypothesis, which suggested a martensitic microstructure based on the observed hardness values. Fig. 10 presents a BF (Bright Field) image within WEL region, with the dotted circle indicating the region that was analyzed.

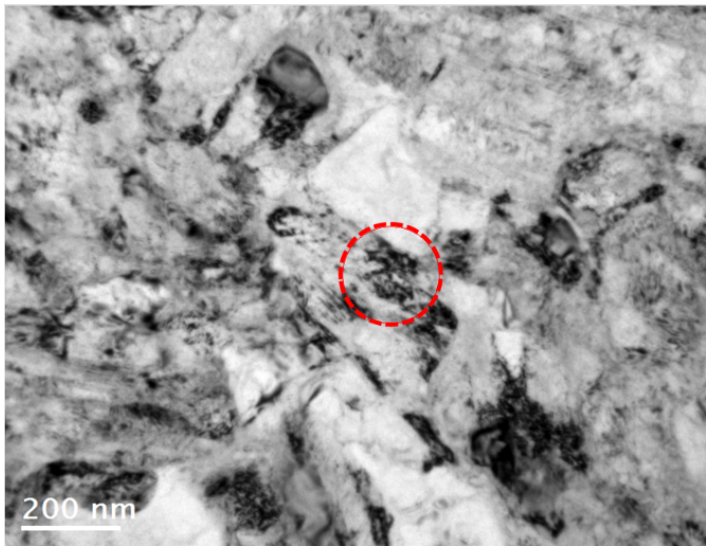

Figure 10. BF(Bright Field) image within WEL region

The diffraction patterns obtained are shown in Fig. 11 and from this the interplanar distance was measures on SAED and compared with theoretical values as it is shown in Table 2

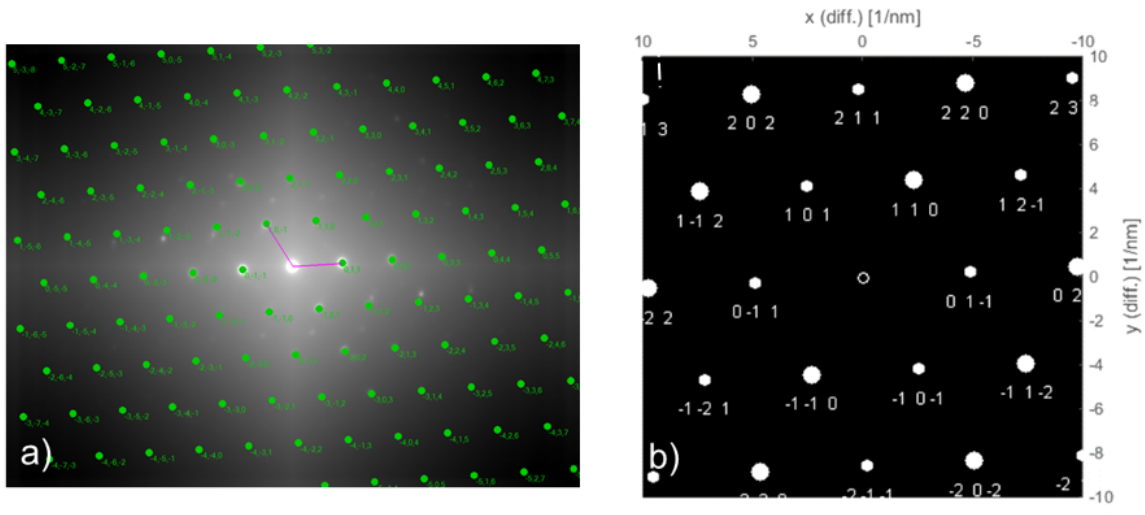

Figure 11. Diffraction patterns of WEL section. a) Pattern Indexing for SAED and b) Simulated SAED Pattern axes zone [-111]

doi: 10.25100/iyc.v27i3.14972

Table 2. Theoretical and experimental d-Spacing

Plane	Theorical d-Spacing[Å]	d-Spacing[Å] (SAED Pattern)
101	2.07050	2.0640
112	1.20740	1.1940
202	1.03540	1.0340
213	0.78930	0.7820

From the data reported in Table 2 above, the preliminary hypothesis was corroborated. The interplanar d-spacing values find in this region are associated with a tetragonal structure related to a martensitic microstructure. The patterns obtain in these analysis point can be related to a martensitic structure which was compared with JCPDS card number # 00-044-1293. These results are supported by the nanoindentation and microhardness values reported in Figures 8 and 9. Microhardness reached up to 900 HV, and nanoindentation hardness reached 12.9 GPa, while Young's modulus values were around 260 GPa. These data confirm a microstructural transformation toward a martensitic structure

Conclusions

It is possible to promote the formation of White Etching Layer and Brown Etching Layer at the surface of pearlitic rails by grinding in laboratory. The mechanical responses of WEL and BEL are different, which may be related to intrinsic microstructural changes in the material as a consequence of the grinding process. It was possible identified by visual inspection the microstructural transformations (WEL and BEL) obtained by grinding process that showed a variation in the contrast and the texture by LOM and SEM techniques in comparison with the pearlitic base material from the ground surface up to 30 microns of depth. The mechanical response of the microstructures identified showed a marked difference with respect to the pearlitic base material by reaching up to three and four times of hardness and nanoindentation values of the bulk respectively. According to the hypothesis based on the mechanical response of the WEL, a martensitic microstructure was confirmed with respect to the diffraction patterns obtained by TEM in the affected zone by comparing the d-spacing with theoretical values

The results of this investigation could be considered as a first stage of a new investigation to use Non-Destructive Techniques for identifications of WEL on rail zones in commercial railways. Also, identifying the operational conditions of the test is possible to study the specific conditions of the WEL generation to reduce this formation during the grinding process as maintenance activity.

Acknowledgements

The authors acknowledge the Servicio Nacional de Aprendizaje SENA for allowing to use its equipment and spaces, the Universidad Nacional de Colombia for funding postdoctoral research, the Metro de Medellín for providing the rail material and Tecnoparque Nodo Medellín for providing equipment for material characterization through the project I2022-0110481-11880.

doi: 10.25100/iyc.v27i3.14972

CrediT authorship contribution statement

Conceptualization - Ideas: Juan C. Sánchez, Jaime A. Jaramillo. Formal analysis: Juan C. Sánchez, Jaime A. Jaramillo. Data curation: Juan C. Sánchez, Jaime A. Jaramillo. Investigation: Juan C. Sánchez. Methodology: Juan C. Sánchez, Jaime A. Jaramillo, Alejandro Toro, Juan C. Sánchez, Project Management: Jaime A. Jaramillo, Hugo A. Estupiñan. Supervision: Juan C. Sánchez, Jaime A. Jaramillo, Alejandro Toro. Hugo A. Estupiñan. Validation: Juan C. Sánchez. Writing - original draft - Preparation: Juan C. Sánchez, Jaime A. Jaramillo. Writing - revision and editing -Preparation: Juan C. Sánchez, Jaime A. Jaramillo, Alejandro Toro, Hugo A. Estupiñan, Luis G. Hernández, Luis V. Wilches.

Financing: Sistema general de regalías-SGR. Conflict of interest: does not declare. Ethical aspect: does not declare.

References

1. Gschwandl TJ, Daves W, Antretter T, Bucher C, Künstner D. On the road towards understanding squats: residual stress state of rails. Procedia Structural Integrity. 2023;46:17-23.

https://doi.org/10.1016/j.prostr.2023.06.004

2. Naseri R, Gedney BL, Asgari H, Rizos DC. Rail squat detection using hybrid processing of axle box acceleration measurements. Results in Engineering. 2025;26:105343.

https://doi.org/10.1016/j.rineng.2025.105343

3. Baltic S, Daves W. Squat initiation mechanism model in a rail-wheel contact. Eng Fract Mech. 2022;269:108525.

https://doi.org/10.1016/j.engfracmech.2022.108525

4. Grassie SL. Studs and squats: The evolving story. Wear. 2016;366-367:194-9.

https://doi.org/10.1016/j.wear.2016.03.021

5. Grassie SL, Fletcher DI, Hernandez EAG, Summers P. Studs: A squat-type defect in rails. Proc Inst Mech Eng F J Rail Rapid Transit. 2012;226(3):243-56.

https://doi.org/10.1177/0954409711421462

6. Xie Y, Ding H, Shi Z, Meli E, Guo J, Liu Q, et al. A novel prediction method for rolling contact fatigue damage of the pearlite rail materials based on shakedown limits and rough set theory with cloud model. Int J Fatigue. 2025;190:108654.

https://doi.org/10.1016/j.ijfatigue.2024.108654

7. Zhao X, Xing YH, Zhang X, Peng F, Xue HD, Han YL. Rail rolling contact fatigue on a Chinese heavy haul line: Observations, monitoring and simulations. Eng Fail Anal. 2025;167:109040.

https://doi.org/10.1016/j.engfailanal.2024.109040

8. Wang R, Tan Z, Tian Y, Zhang J, Gao Y, Shan A, et al. Study on rolling contact fatigue crack initiation and propagation in U75V rail treated by laminar plasma. Tribol Int. 2024;198:109879.

https://doi.org/10.1016/j.triboint.2024.109879

9. Yang J, Huo J, Yao D. Rail corrugation detection based on optimal position window and Weighted-bandwidth mode decomposition. Measurement. 2025;255:117888.

doi: 10.25100/iyc.v27i3.14972

https://doi.org/10.1016/j.measurement.2025.117888

10. Zhang P, Li S, Ren F, Hajizad O, Dollevoet R, Li Z. Microstructural investigation into the damage mechanism of short pitch rail corrugation. Eng Fail Anal. 2025;174:109512.

https://doi.org/10.1016/j.engfailanal.2025.109512

11. Guan Q, Wen Z, Liu B, Wang H, Liang S. A new perspective on rail corrugation and its practical implications. Wear. 2025;564-565:205743.

https://doi.org/10.1016/j.wear.2025.205743

12. Bedoya-Zapata AD, León-Henao H, Mesaritis M, Molina LF, Palacio M, Santa JF, et al. White Etching Layer (WEL) formation in different rail grades after grinding operations in the field. Wear. 2022;502-503:204371.

https://doi.org/10.1016/j.wear.2022.204371

13. Liu JP, Huang H, Liu A, Ma SN, Ren Y, Ding HH, et al. Formation mechanism of white etching layers in pearlitic rail steels under continuous abrasion. Wear. 2025;572-573:206050.

https://doi.org/10.1016/j.wear.2025.206050

14. Saxena AK, Kumar A, Herbig M, Brinckmann S, Dehm G, Kirchlechner C. Micro fracture investigations of white etching layers. Mater Des. 2019;180:107892.

https://doi.org/10.1016/j.matdes.2019.107892

15. Ding HH, Fu ZK, Wang WJ, Guo J, Liu QY, Zhu MH. Investigation on the effect of rotational speed on rolling wear and damage behaviors of wheel/rail materials. Wear. 2015;330-331:563-70.

https://doi.org/10.1016/j.wear.2014.12.043

16. Chang C, Chen B, Cai Y, Wang J. Experimental investigation of high-speed wheel-rail adhesion characteristics under large creepage and water conditions. Wear. 2024;540-541:205254.

https://doi.org/10.1016/j.wear.2024.205254

17. Hu Y, Zhou L, Ding HH, Tan GX, Lewis R, Liu QY, et al. Investigation on wear and rolling contact fatigue of wheel-rail materials under various wheel/rail hardness ratio and creepage conditions. Tribol Int. 2020;143:106091.

https://doi.org/10.1016/j.triboint.2019.106091

18. Zhang SY, Feng ZJ, Wang WJ, Zhao HY, Ding HH, Liu QY, et al. Effects of varying normal loads on the rail rolling contact fatigue behavior under various frequencies and creepages. Wear. 2023;520-521:204670.

https://doi.org/10.1016/j.wear.2023.204670

19. Schotsman B, Huisman J, Santofimia MJ, Petrov RH, Sietsma J. Microstructure evolution and damage development in the rails of a single-track railway line after preventive grinding. Wear. 2025;576-577:206101.

https://doi.org/10.1016/j.wear.2025.206101

20. Han ZY, Wang HH, Wang WJ, Zhang SY, Lin DM, Wang Y, et al. The correlation between material deformed microstructure and rolling contact fatigue crack propagation of U71Mn rail when matching with CL60 wheel. Tribol Int. 2024;200:110069.

https://doi.org/10.1016/j.triboint.2024.110069

21. Zhang X, Wu D, Xia Z, Zhang Y, Li Y, Wang J, et al. Microstructure characteristics and formation mechanisms of white etching layer (WEL) and brown etching layer (BEL) on martensite bearing raceway. Journal of Materials Research and Technology. 2023;25:4876-87.

https://doi.org/10.1016/j.jmrt.2023.06.217

22. Al-Juboori A, Li H, Zhu H. Formation of white etching layer on rails due to coupled thermal and mechanical actions. Wear. 2023;530-531:205063.

https://doi.org/10.1016/j.wear.2023.205063

23. Thiercelin L, Saint-Aimé L, Lebon F, Saulot A. Thermomechanical modelling of the tribological surface transformations in the railroad network (white etching layer). Mechanics of Materials. 2020;151(October):103636.

https://doi.org/10.1016/j.mechmat.2020.103636

24. Pena LVW, Wang L, Mellor BG, Huang Y. White etching structures in annealed 52100 bearing steel arising from high-pressure torsion tests. Tribol Int. 2021;164:107187.

https://doi.org/10.1016/j.triboint.2021.107187

25. Wan LB, Li SX, Lu SY, Su YS, Shu XD, Huang HB. Case study: Formation of white etching layers in a failed rolling element bearing race. Wear. 2018;396-397(July 2017):126-34.

https://doi.org/10.1016/j.wear.2017.07.014

26. Li JG, Umemoto M, Todaka Y, Tsuchiya K. A microstructural investigation of the surface of a drilled hole in carbon steels. Acta Mater. 2007;55(4):1397-406.

https://doi.org/10.1016/j.actamat.2006.09.043

27. Hosseini SB, Beno T, Klement U, Kaminski J, Ryttberg K. Cutting temperatures during hard turning-Measurements and effects on white layer formation in AISI 52100. J Mater Process Technol. 2014;214(6):1293-300.

https://doi.org/10.1016/j.jmatprotec.2014.01.016

28. Al-Juboori A, Zhu H, Li H, McLeod J, Pannila S, Barnes J. Microstructural investigation on a rail fracture failure associated with squat defects. Eng Fail Anal. 2023;151:107411.

https://doi.org/10.1016/j.engfailanal.2023.107411

29. Talebi N, Andersson B, Ekh M, Meyer KA. Influence of a highly deformed surface layer on RCF predictions for rails in service. Wear. 2025;578-579:206173.

https://doi.org/10.1016/j.wear.2025.206173

30. Liu J, Ou J, Li J, Yu Z, He C, Li P, et al. Initiation and propagation mechanism of fish-scale-like fatigue cracks on a U75V quenched rail. Eng Fail Anal. 2025;174:109468.

https://doi.org/10.1016/j.engfailanal.2025.109468

31. Edjeou W, P.-O. L, Larsson R, A A. Effect of the rail surface topography on wear and fatigue. Wear. 2025;206218.

https://doi.org/10.1016/j.wear.2025.206218

32. Kanematsu Y, Uehigashi N, Matsui M, Noguchi S. Influence of a decarburised layer on the formation of microcracks in railway rails: On-site investigation and twin-disc study. Wear. 2022;504-505:204427.

https://doi.org/10.1016/j.wear.2022.204427

doi: 10.25100/iyc.v27i3.14972

33. Tosangthum N, Krataitong R, Wila P, Koiprasert H, Buncham K, Kansuwan P, et al. Dry rolling-sliding wear behavior of ER9 wheel and R260 rail couple under different operating conditions. Wear. 2023;518-519:204636.

https://doi.org/10.1016/j.wear.2023.204636

34. Carroll RI, Beynon JH. Rolling contact fatigue of white etching layer: Part 1. Crack morphology. Wear. 2007;262(9-10):1253-66.

https://doi.org/10.1016/j.wear.2007.01.003

35. Grassie SL. Squats and squat-type defects in rails: The understanding to date. Proc Inst Mech Eng F J Rail Rapid Transit. 2012;226(3):235-42.

https://doi.org/10.1177/0954409711422189

36. Österle W, Rooch H, Pyzalla A, Wang L. Investigation of white etching layers on rails by optical microscopy, electron microscopy, X-ray and synchroton X-ray diffraction. Materials Science and Engineering A. 2001;303(1-2):150-7.

https://doi.org/10.1016/S0921-5093(00)01842-6

37. Lojkowski W, Djahanbakhsh M, Bürkle G, Gierlotka S, Zielinski W, Fecht HJ. Nanostructure formation on the surface of railway tracks. Materials Science and Engineering A. 2001;

https://doi.org/10.1016/S0921-5093(00)01947-X

38. Zhang HW, Ohsaki S, Mitao S, Ohnuma M, Hono K. Microstructural investigation of white etching layer on pearlite steel rail. Materials Science and Engineering: A. 2006;421(1):191-9.

https://doi.org/10.1016/j.msea.2006.01.033

39. Wu J, Petrov RH, Naeimi M, Li Z, Dollevoet R, Sietsma J. Laboratory simulation of martensite formation of white etching layer in rail steel. Int J Fatigue. 2016;91:11-20.

https://doi.org/10.1016/j.ijfatigue.2016.05.016

40. Takahashi J, Kawakami K, Ueda M. Atom probe tomography analysis of the white etching layer in a rail track surface. Acta Mater. 2010;58(10):3602-12.

https://doi.org/10.1016/j.actamat.2010.02.030

41. Masoumi M, Lima NB De, Tressia G, Sinatora A, Goldenstein H. Microstructure and crystallographic orientation evolutions below the superficial white layer of a used pearlitic rail. Journal of Materials Research and Technology. 2019;8(6):6275-88.

https://doi.org/10.1016/j.jmrt.2019.10.021

42. Newcomb SB, Stobbs WM. A transmission electron microscopy study of the white-etching layer on a rail head. Materials Science and Engineering. 1984;66(2):195-204.

https://doi.org/10.1016/0025-5416(84)90180-0

43. Baumann G, Fecht HJ, Liebelt S. Formation of white-etching layers on rail treads. Wear. 1996;191(1-2):133-40.

https://doi.org/10.1016/0043-1648(95)06733-7

44. Jaramillo J, Sánchez JC, Suárez-Bustamante FA, Vargas D, Vargas G, Toro A, et al. Implementation of the Magnetic Barkhausen Noise Technique for Microstructural Characterization of Rail Steel. J Nondestr Eval. 2025;44(2):42.

https://doi.org/10.1007/s10921-025-01184-y

doi: 10.25100/iyc.v27i3.14972

45. Li S, Wu J, Petrov RH, Li Z, Dollevoet R, Sietsma J. "Brown etching layer": A possible new insight into the crack initiation of rolling contact fatigue in rail steels? Eng Fail Anal. 2016;66:8-18.

https://doi.org/10.1016/j.engfailanal.2016.03.019

46. Wang L. Microstructure and Residual Stress State in the Contact Zone of Rails and Wheels. 2002.

47. Steenbergen M, Dollevoet R. On the mechanism of squat formation on train rails - Part I: Origination. Int J Fatigue. 2013;47:361-72.

https://doi.org/10.1016/j.ijfatigue.2012.04.023

48. Thiercelin L, Cazottes S, Saulot A, Lebon F, Mercier F, Le Bourlot C, et al. Development of Temperature-Controlled Shear Tests to Reproduce White-Etching-Layer Formation in Pearlitic Rail Steel. Materials. 2022 Oct 1;15(19).

https://doi.org/10.3390/ma15196590

49. Liu JP, Huang H, Liu A, Ma SN, Ren Y, Ding HH, et al. Formation mechanism of white etching layers in pearlitic rail steels under continuous abrasion. Wear. 2025 Jul 1;572-573.

https://doi.org/10.1016/j.wear.2025.206050

50. Zhou Y, Peng JF, Luo ZP, Cao BB, Jin XS, Zhu MH. Phase and microstructural evolution in white etching layer of a pearlitic steel during rolling-sliding friction. Wear. 2016;362-363:8-17.

https://doi.org/10.1016/j.wear.2016.05.007

51. Kumar A, Agarwal G, Petrov R, Goto S, Sietsma J, Herbig M. Microstructural evolution of white and brown etching layers in pearlitic rail steels. Acta Mater. 2019;171:48-64.

https://doi.org/10.1016/j.actamat.2019.04.012

52. Baumann G, Zhong Y, Fecht HJ. Comparison between nanophase formation during friction induced surface wear and mechanical attrition of a pearlitic steel. Nanostructured Materials. 1996;7(1):237-44.

https://doi.org/10.1016/0965-9773(96)00305-4

53. Schotsman B, Huisman J, Santofimia MJ, Petrov RH, Sietsma J. Microstructure evolution and damage development in the rails of a single-track railway line after preventive grinding. Wear. 2025 Aug 15;576-577.

https://doi.org/10.1016/j.wear.2025.206101

54. Russo M, Saulot A, Sauvage X, Véron M, Rauch E, Thiercelin L, et al. Multiscale microstructural investigations of white and brown etching layers initiating the squat formation in pearlitic rail steels. Mater Charact. 2025 Nov 1;229.

https://doi.org/10.1016/j.matchar.2025.115477

55. Hieu Nguyen B, Al-Juboori A, Zhu H, Zhu Q, Li H, Tieu K. Formation mechanism and evolution of white etching layers on different rail grades. Int J Fatigue. 2022 Oct 1;163.

https://doi.org/10.1016/j.ijfatigue.2022.107100

56. Al-Juboori A, Li H, Zhu H. Formation of white etching layer on rails due to coupled thermal and mechanical actions. Wear. 2023 Oct 15;530-531.

https://doi.org/10.1016/j.wear.2023.205063